

# Weierstraß-Institut für Angewandte Analysis und Stochastik

im Forschungsverbund Berlin e.V.

Preprint

ISSN 0946 – 8633

## Surface waves on permeable and impermeable boundaries of poroelastic media

Bettina Albers

submitted: 17th January 2005

Weierstrass Institute  
for Applied Analysis  
and Stochastics  
Mohrenstrasse 39  
10117 Berlin  
Germany  
E-Mail: [albers@wias-berlin.de](mailto:albers@wias-berlin.de)

No. 1002  
Berlin 2005



---

2000 *Mathematics Subject Classification.* 74J15, 76S05, 74S99.

*Key words and phrases.* Surface waves, flows in porous media, numerical analysis of dispersion relation.

Edited by  
Weierstraß-Institut für Angewandte Analysis und Stochastik (WIAS)  
Mohrenstraße 39  
10117 Berlin  
Germany

Fax: + 49 30 2044975  
E-Mail: [preprint@wias-berlin.de](mailto:preprint@wias-berlin.de)  
World Wide Web: <http://www.wias-berlin.de/>

**ABSTRACT:** This work is devoted to the numerical analysis of surface waves in two-component saturated poroelastic media. We use the "simple mixture model" which is a simplification of the classical Biot's model for poroelastic media.

For the interface porous medium/vacuum there exist two surface waves in the whole range of frequencies – a leaky Rayleigh wave and a true Stoneley wave. For the interface porous medium/fluid one more surface wave appears – a leaky Stoneley wave. For this boundary velocities and attenuations of the waves are shown in dependence on the surface permeability. The true Stoneley wave exists only in a limited range of this parameter.

## 1 INTRODUCTION

The theoretical investigation of surface waves in porous materials is motivated by the possible construction of a method of nondestructive testing of materials. Different operational areas require very different regions of frequencies of the waves: e.g. for field measurements in soil mechanics the range of applicable frequencies lies between 1 Hz and 100 Hz while testing of nanomaterials requires frequencies of approx. 100 MHz. Therefore we investigate the dispersion relation in the whole range of frequencies.

Apart from the frequency range, the acoustic parameters are also investigated in dependence on two other parameters. One of them is the bulk permeability of the porous material,  $\pi$ . Furthermore the properties of the boundary are described by the surface permeability,  $\alpha$ . It controls the intensity of the in- and outflow of the fluid from the porous medium.

## 2 SIMPLE MIXTURE MODEL

In our analysis we rely on a simpler model than this of Biot. We neglect two effects:

- the added mass effect reflected in Biot's model by off-diagonal contributions to the matrix of partial mass densities (the parameter  $\rho_{12}$ ),
- the static coupling effect between partial stresses (the parameter  $Q$ ).

The first one is neglected because it yields a non-objectivity of Biot's equations (Wilmanski 2004).

The second contribution, the coupling of partial stresses  $Q$ , is neglected because it yields at most

*quantitative* corrections without changing the *qualitative* behavior of the system, at least in the range of a relatively high stiffness of the skeleton in comparison with the fluid. This has been analyzed for bulk waves in (Albers and Wilmanski 2003b).

Bearing these remarks in mind it seems to be appropriate to rely on the simplified model ("simple mixture model" in which  $Q = 0$ ,  $\rho_{12} = 0$ ). It has the advantage to reduce essentially technical difficulties.

We present here the linear form of the "simple mixture" model for a two-component poroelastic saturated medium (for details see: (Wilmanski 1999)).

In the simple mixture model a process is described by the *macroscopic* fields  $\rho^F(\mathbf{x}, t)$ , the partial mass density of the fluid,  $\mathbf{v}^F(\mathbf{x}, t)$ ,  $\mathbf{v}^S(\mathbf{x}, t)$ , the velocities of the fluid and of the skeleton, respectively,  $\mathbf{e}^S(\mathbf{x}, t)$ , the symmetric tensor of small deformations of the skeleton and  $n$ , the porosity. The following set of linear equations is satisfied by those fields

$$\begin{aligned} \frac{\partial \rho^F}{\partial t} + \rho_0^F \operatorname{div} \mathbf{v}^F &= 0, \quad \left| \frac{\rho^F - \rho_0^F}{\rho_0^F} \right| \ll 1, \\ \rho_0^F \frac{\partial \mathbf{v}^F}{\partial t} + \kappa \operatorname{grad} \rho^F + \beta \operatorname{grad} \Delta + \hat{\mathbf{p}} &= 0, \quad (1) \\ \rho_0^S \frac{\partial \mathbf{v}^S}{\partial t} - \operatorname{div} (\lambda^S (\operatorname{tr} \mathbf{e}^S) \mathbf{1} + 2\mu \mathbf{e}^S + \beta \Delta \mathbf{1}) - \\ &\quad - \hat{\mathbf{p}} = 0, \\ \hat{\mathbf{p}} &:= \pi (\mathbf{v}^F - \mathbf{v}^S), \quad \Delta := n - n_E, \end{aligned}$$

$$\frac{\partial \mathbf{e}^S}{\partial t} = \text{sym grad } \mathbf{v}^S, \quad \|\mathbf{e}^S\| \ll 1, \quad (1)_{\text{cont.}}$$

$$\frac{\partial \Delta}{\partial t} + \Phi \text{div} (\mathbf{v}^F - \mathbf{v}^S) + \frac{\Delta}{\tau_n} = 0,$$

$$n_E := n_0 (1 + \delta \text{tr } \mathbf{e}^S), \quad \left| \frac{n - n_0}{n_0} \right| \ll 1.$$

In these relations  $\rho_0^F, \rho_0^S, n_0$  are the constant reference values of partial mass densities, and porosity, respectively. There appear constant material parameters  $\kappa, \lambda^S, \mu^S, \beta, \pi, \tau_n, \delta, \Phi$ . In particular,  $\kappa$  denotes the macroscopic compressibility of the fluid component,  $\lambda^S$  and  $\mu^S$  are macroscopic elastic constants of the skeleton,  $\beta$  is the coupling constant between the components,  $\pi$  denotes the bulk permeability coefficient,  $\tau_n$  describes the relaxation time of porosity and  $\delta, \Phi$  are material parameters related to equilibrium and nonequilibrium changes of porosity, respectively. As already done in the works (Albers 2005) and (Albers and Wilmanski 2003a) for the analysis of surface waves the coupling parameter  $\beta$  is assumed to be zero. Then the problem of evolution of porosity can be solved separately from the rest of the problem.

The additional equations for the fluid in the exterior of the porous material read

$$\begin{aligned} \frac{\partial \rho^{F+}}{\partial t} + \rho_0^{F+} \text{div } \mathbf{v}^{F+} &= 0, \\ \rho_0^{F+} \frac{\partial \mathbf{v}^{F+}}{\partial t} + \kappa^+ \text{grad } \rho^{F+} &= 0. \end{aligned} \quad (2)$$

The quantities outside of the porous medium are denoted by a "+" sign. Thus  $\rho^{F+}$  denotes the partial mass density of the fluid in the + -region and  $\rho_0^{F+}$  is its constant reference value.  $\kappa^+$  describes the true compressibility of the fluid.

### 3 BOUNDARY CONDITIONS

For the determination of surface waves in saturated poroelastic media conditions for  $z = 0$  are needed. Boundary conditions for the interface between a saturated porous material and an ideal fluid were formulated by Deresiewicz & Skalak (Deresiewicz and Skalak 1963). In a slightly changed notation they have the following form

- $(T_{13} - T_{13}^+) \Big|_{z=0} \equiv T_{13}^S \Big|_{z=0} =$   
 $= c_S^2 \rho_0^S \left( \frac{\partial u_1^S}{\partial z} + \frac{\partial u_3^S}{\partial x} \right) \Big|_{z=0} = 0, \quad (3)$
- $(T_{33} - T_{33}^+) \Big|_{z=0} \equiv (T_{33}^S + p^{F+} - p^F) \Big|_{z=0} =$

$$\begin{aligned} &= c_{P1}^2 \rho_0^S \left( \frac{\partial u_1^S}{\partial x} + \frac{\partial u_3^S}{\partial z} \right) - 2c_S^2 \rho_0^S \frac{\partial u_1^S}{\partial x} + \\ &+ c_+^2 (\rho^{F+} - \rho_0^{F+}) - \\ &- c_{P2}^2 (\rho^F - \rho_0^F) \Big|_{z=0} = 0, \end{aligned}$$

- $\rho_0^F \frac{\partial}{\partial t} (u_3^F - u_3^S) \Big|_{z=0} =$   
 $= \rho_0^{F+} \frac{\partial}{\partial t} (u_3^{F+} - u_3^S) \Big|_{z=0}, \quad (3)_{\text{cont.}}$
- $\rho_0^F \frac{\partial}{\partial t} (u_3^F - u_3^S) + \alpha (p^F - n_0 p^{F+}) \Big|_{z=0} = 0.$

Here  $u_1^S, u_3^S$  are  $x$ -, and  $z$ -components of the displacement  $\mathbf{u}^S$ , respectively, and  $u_3^F, u_3^{F+}$  denote  $z$ -components of the displacements  $\mathbf{u}^F$  and  $\mathbf{u}^{F+}$ , respectively. Simultaneously,  $c_{P1}^2 := (\lambda^S + 2\mu^S)/\rho_0^S$ ,  $c_S^2 := \mu^S/\rho_0^S$ ,  $c_{P2}^2 := \kappa$  and  $c_+^2 := \kappa^+$  are squares of the front velocities of bulk waves in the porous material:  $P1$  (fast wave),  $S$  (shear wave),  $P2$  (slow wave, also called Biot's wave), and of the  $P$ -wave in the fluid, respectively. In the case of Biot's model there would be an additive contribution of the coupling parameter  $Q$  in the numerator of  $c_{P1}$  which is of the order of a few percent of  $\lambda^S$  (see: (Albers and Wilmanski 2003b) for a detailed analysis).

Two of the boundary conditions,  $(3)_1$  and  $(3)_2$ , describe the continuity of the full traction,  $\mathbf{t} := (\mathbf{T}^S + \mathbf{T}^F) \mathbf{n}$ ,  $\mathbf{n} = (0, 0, 1)^T$ , on the boundary;  $(3)_3$  reflects the continuity of the fluid mass flux, and condition  $(3)_4$  specifies the mass transport through the surface. The difference of the pore pressures on both sides of the boundary determines the in- and outflow through the boundary.  $\alpha$  denotes a surface permeability coefficient, which corresponds to  $\frac{1}{T}$  in the works (Feng and Johnson 1983), (Gubaidullin et al. 2004), and  $p^{F+}$  is the external pressure. Condition  $(3)_4$  relies on the assumption that the pore pressure  $p$  and the partial pressure  $p^F$  satisfy the relation  $p^F \approx n_0 p$  at least in a small vicinity of the surface.

For the boundary porous medium/vacuum is  $\alpha = 0$  and also the quantities outside of the porous medium are equal to zero. Then the third and the fourth conditions are identical.

### 4 SOLUTION OF THE PROBLEM

We consider monochromatic waves with a given *real frequency*  $\omega$ . The construction of the solution for some problems was shown already in earlier works (see e.g. (Wilmanski and Albers 2003), (Albers and

Wilmanski 2003a) or (Albers 2005)) therefore we do not show it here but give an impression how it was done.

We have introduced displacement vectors for the three components using potentials. In the two-dimensional case for those potentials monochromatic wave solutions in the  $x$ -direction (exponential ansatz) have been assumed. The solutions have been substituted in the field equations of the simple mixture model. This has led to seven compatibility conditions containing some unknown coefficients. A dimensionless notation has been introduced. This has the advantage to connect characteristics of the surface waves to those of the better known bulk waves (e.g. with the velocity of the  $P1$ -wave  $c_{P1}$ ). The dimensionless quantities are defined as

$$\begin{aligned} c_s &:= \frac{c_S}{c_{P1}}, & c_f &:= \frac{c_{P2}}{c_{P1}}, & c_f^+ &:= \frac{\sqrt{\kappa^+}}{c_{P1}}, \\ k' &:= k c_{P1} \tau, & \omega' &:= \omega \tau, & \pi' &:= \frac{\pi \tau}{\rho_0^S}, \\ \alpha' &:= \alpha c_{P1}, & r &:= \frac{\rho_0^F}{\rho_0^S}, & r^+ &:= \frac{\rho_0^{F+}}{\rho_0^S}, \\ z' &:= \frac{z}{c_{P1} \tau}. \end{aligned} \quad (4)$$

Here  $\tau$  is an arbitrary reference time. We further use the dimensionless quantities omitting the prime. Substitution of these quantities into the compatibility conditions yields for the boundary porous medium/fluid four equations, for the boundary porous medium/vacuum three equations still containing unknown coefficients. However, in contrast to heterogeneous media, they are for homogeneous materials independent of  $z$ . This leads to a differential eigenvalue problem which can be easily solved. We seek solutions in exponential form. In these relations the exponents  $\gamma_1, \gamma_2, \zeta$  must possess negative real parts and  $\gamma^+$  must possess a positive real part to describe a surface wave. We obtain relations for the exponents:

$\frac{\zeta_{1,2}}{k}$  follow from

$$\left(\frac{\zeta}{k}\right)^2 = 1 - \frac{1}{c_s^2} \left(1 + \frac{i\pi}{\omega + i\frac{\pi}{r}}\right) \left(\frac{\omega}{k}\right)^2, \quad (5)$$

$\frac{\gamma_{1,2,3,4}}{k}$  result as solutions of the relation

$$\begin{aligned} c_f^2 \left[\left(\frac{\gamma}{k}\right)^2 - 1\right]^2 + \left[1 + \left(1 + \frac{1}{r}\right) \frac{i\pi}{\omega}\right] \left(\frac{\omega}{k}\right)^4 + \\ + \left[1 + c_f^2 + \left(c_f^2 + \frac{1}{r}\right) \frac{i\pi}{\omega}\right] \left[\left(\frac{\gamma}{k}\right)^2 - 1\right] \left(\frac{\omega}{k}\right)^2 = 0, \end{aligned} \quad (6)$$

and  $\frac{\gamma_{1,2}^+}{k}$  as solutions of

$$\left(\frac{\gamma^+}{k}\right)^2 = 1 - \frac{1}{c_f^{+2}} \left(\frac{\omega}{k}\right)^2. \quad (7)$$

However, the unknown constants have still to be determined by the boundary conditions. We use the constitutive relations

$$\begin{aligned} p^F &= p_0^F + \kappa (\rho^F - \rho_0^F), \\ p^{F+} &= p_0^{F+} + \kappa^+ (\rho^{F+} - \rho_0^{F+}), \end{aligned} \quad (8)$$

and assume

$$p_0^{F+} = \frac{p_0^F}{n_0}, \quad n_0 = \frac{r}{r^+} \text{ if } r^+ \neq 0. \quad (9)$$

The first condition means that the initial external pressure is equal to the initial pore pressure. After insertion into the boundary conditions we obtain the following eigenvalue problem

$$\mathbf{A}\mathbf{X} = \mathbf{0}, \quad (10)$$

where

$$\mathbf{A} := \begin{pmatrix} \left(\frac{\zeta}{k}\right)^2 + 1 & -2i\frac{\gamma_1}{k} \\ 2ic_s^2 \frac{\zeta}{k} & \left(\frac{\gamma_1}{k}\right)^2 - 1 + 2c_s^2 + r c_f^2 \left[\left(\frac{\gamma_1}{k}\right)^2 - 1\right] \delta_f \\ -\frac{\pi}{r\omega + i\pi} + i\left(\frac{r^+}{r} - 1\right) & \frac{\gamma_1}{k} \left[\delta_f + \left(\frac{r^+}{r} - 1\right)\right] \\ \frac{r\omega}{r\omega + i\pi} \frac{\omega}{k} & i\frac{\omega}{k} \frac{\gamma_1}{k} (\delta_f - 1) + \alpha c_f^2 \left[\left(\frac{\gamma_1}{k}\right)^2 - 1\right] \delta_f \end{pmatrix} \quad (11)$$

$$\mathbf{X} := \begin{pmatrix} -2i\frac{\gamma_2}{k} \delta_s & 0 \\ \left[\left(\frac{\gamma_2}{k}\right)^2 - 1 + 2c_s^2\right] \delta_s + r c_f^2 \left[\left(\frac{\gamma_2}{k}\right)^2 - 1\right] & -r^+ c_f^{+2} \left[\left(\frac{\gamma^+}{k}\right)^2 - 1\right] \\ \frac{\gamma_2}{k} \left[1 + \delta_s \left(\frac{r^+}{r} - 1\right)\right] & -\frac{r^+}{r} \frac{\gamma^+}{k} \\ i\frac{\omega}{k} \frac{\gamma_2}{k} (1 - \delta_s) + \alpha c_f^2 \left[\left(\frac{\gamma_2}{k}\right)^2 - 1\right] & -\alpha c_f^{+2} \left[\left(\frac{\gamma^+}{k}\right)^2 - 1\right] \end{pmatrix}^T, \quad (12)$$

and auxiliary quantities

$$\begin{aligned} \delta_f &:= \frac{1}{r} \frac{\frac{i\pi}{\omega} \frac{\omega^2}{k^2}}{c_f^2 \left[\left(\frac{\gamma_1}{k}\right)^2 - 1\right] + \left(\frac{\omega}{k}\right)^2 + \frac{i\pi}{\omega r} \frac{\omega^2}{k^2}}, \\ \delta_s &:= \frac{\frac{i\pi}{\omega} \frac{\omega^2}{k^2}}{\left(\frac{\gamma_2}{k}\right)^2 - 1 + \left(\frac{\omega}{k}\right)^2 + \frac{i\pi}{\omega} \frac{\omega^2}{k^2}}. \end{aligned} \quad (13)$$

This homogeneous set yields the *dispersion relation*:  $\det \mathbf{A} = 0$  determining the relation between  $\omega$  and  $k$ .

## 5 PARAMETERS, NUMERICAL PROCEDURE

For both boundaries the problem  $\det \mathbf{A} = 0$  has been solved for the complex wave number,  $k$ , using the two computing packages MAPLE and MATLAB. It is possible to use the existing equation solvers although they need for calculations with complex variables a very extensive main memory.

The calculations have been performed for the following data which correspond to water saturated sandstones:

Table 1. Parameters for water saturated sandstones.

For both boundaries:		
$\beta = 0,$	$c_{P1} = 2500 \frac{\text{m}}{\text{s}},$	$c_{P2} = 1000 \frac{\text{m}}{\text{s}},$
$\rho_0^S = 2500 \frac{\text{kg}}{\text{m}^3},$	$\rho_0^F = 250 \frac{\text{kg}}{\text{m}^3},$	$r = \frac{\rho_0^F}{\rho_0^S} = 0.1,$
$c_f = \frac{c_{P2}}{c_{P1}} = 0.4,$	$\tau = \tau_n = 10^{-6} \text{ s},$	
For the boundary porous medium/vacuum:		
$c_S = 1500 \frac{\text{m}}{\text{s}},$	$c_s = \frac{c_S}{c_{P1}} = 0.6,$	
For the boundary porous medium/fluid:		
$c_S = 1250 \frac{\text{m}}{\text{s}},$	$c_s = \frac{c_S}{c_{P1}} = 0.4,$	$\rho_0^{F+} = 1000 \frac{\text{kg}}{\text{m}^3},$
$c_+ = 1500 \frac{\text{m}}{\text{s}},$	$c_f^+ = \frac{c_+}{c_{P1}} = 0.6,$	$r^+ = \frac{\rho_0^{F+}}{\rho_0^S} = 0.4.$

## 6 RESULTS

### 6.1 Boundary porous medium/vacuum

In the whole range of frequencies there exist two surface waves corresponding to the classical Rayleigh and Stoneley waves. The results for the phase velocities and attenuations are shown for different values of the bulk permeability coefficient,  $\pi$ . This parameter describes the resistance of the porous medium against the flow of the fluid. Figures 1 and 2 show the phase velocities of the Rayleigh and Stoneley waves in dependence on the frequency. They are normalized by the  $P1$ -velocity. We see a range of frequencies from zero to the very large value of 100 MHz. Certainly, all values lie below the normalized velocity of the shear wave  $c_s \equiv \frac{c_S}{c_{P1}} = 0.6$ .

The Stoneley velocity increases from the zero value for  $\omega = 0$ . The growth is faster than the growth of the Rayleigh velocity but the maximum value is smaller. It lies always below the normalized velocity of the fluid  $c_f \equiv \frac{c_{P2}}{c_{P1}} = 0.4$ . The maximum value of the Stoneley velocity appearing for  $\omega \rightarrow \infty$  is approximately 0.15% smaller than the velocity of the fluid.

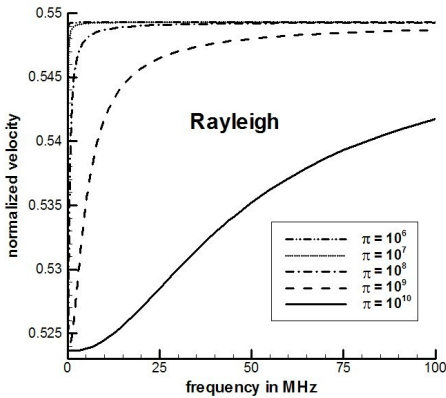


Figure 1: Boundary porous medium/vacuum. Normalized velocity of the leaky Rayleigh wave in dependence on the frequency and the surface permeability.

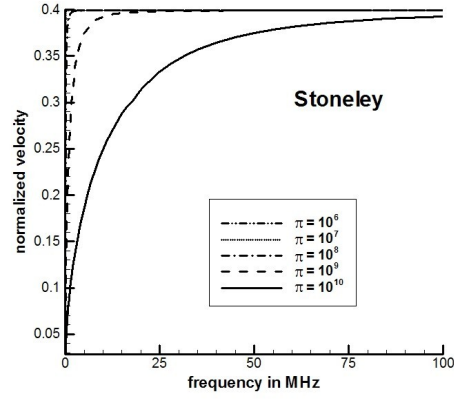


Figure 2: Boundary porous medium/vacuum. Normalized velocity of the true Stoneley wave in dependence on the frequency and the surface permeability.

One should point out that – differently than often stated – the Stoneley velocity behaves regularly in the whole range of frequencies and it ceases to exist only for  $\omega = 0$ . In the vicinity of this point the Stoneley velocity possesses a similar feature to the  $P2$ -wave: it decays to zero as  $\sqrt{\omega}$ . Imaginary parts of the wave number  $k$  determine the damping of waves. It is normalized by the product with the  $P1$ -velocity and the relaxation time. Figure 3 shows the attenuation of the Rayleigh wave. It is obvious that this wave is strongly attenuated. The attenuation linearly increases to infinity as  $\omega \rightarrow \infty$ , i.e. the Rayleigh wave is leaky. Similar to the attenuation of  $P1$ -waves these curves intersect for different values of  $\pi$ . The attenuation for all values of  $\pi$  starts from zero.

Figure 4 shows that also the normalized attenuation of the Stoneley wave starts from the zero value for  $\omega = 0$ . But in contrast to the Rayleigh wave attenuation for small frequencies it increases much faster and then approaches a horizontal asymptotic value for larger values of the frequency. This means the limit  $\omega \rightarrow \infty$  is finite and dependent on the permeability coefficient  $\pi$ .

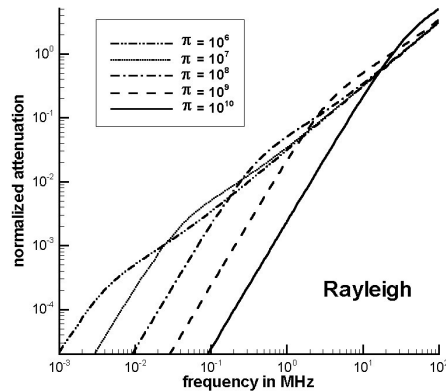


Figure 3: Boundary porous medium/vacuum. Normalized attenuation of the leaky Rayleigh wave in dependence on the frequency and the surface permeability.

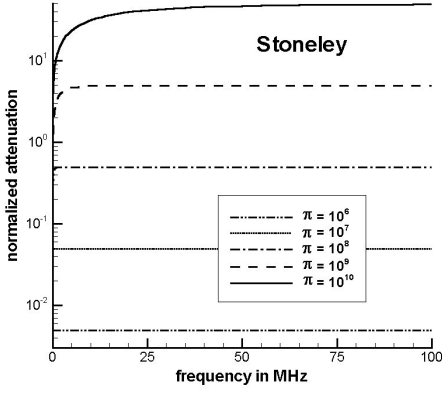


Figure 4: Boundary porous medium/vacuum. Normalized attenuation of the Stoneley wave in dependence on the frequency and the surface permeability.

### 6.2 Boundary porous medium/fluid

Figures 5 to 10 show the phase velocities and the attenuations of all three surface waves appearing at the interface between a porous halfspace and a fluid halfspace. Also here we show the wide range of frequencies between 1 Hz and 100 MHz. The curves depend on the frequency and on the surface permeability parameter  $\alpha$ .  $\alpha = 0$  means that the surface is completely impermeable while  $\alpha = \infty$  corresponds to an open pore situation. Both the frequency and the attenuations are shown in logarithmic scale while the velocity is presented in normal scale. Again, the velocity of the Rayleigh wave lies under the velocity of the bulk shear wave,  $c_S$ , whose normalized value is now  $c_s \equiv \frac{c_S}{c_{P1}} = 0.5$ . While for small frequencies the velocity is independently of  $\alpha$ , the high frequency limit decreases with increasing  $\alpha$ . For the open pore situation the difference between high and low frequency limits is approximately one half of the difference for a close boundary. For frequencies around 100 kHz there is a steep increase of the Rayleigh velocity. For small values of  $\alpha$  there appears a small plateau in the frequency

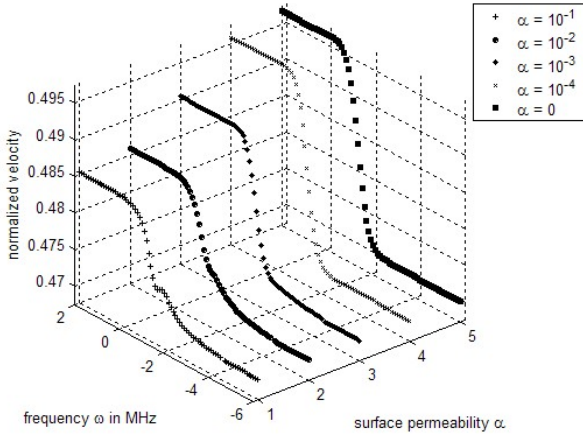


Figure 5: Boundary porous medium/fluid. Normalized velocity of the leaky Rayleigh wave in dependence on the frequency and the surface permeability.

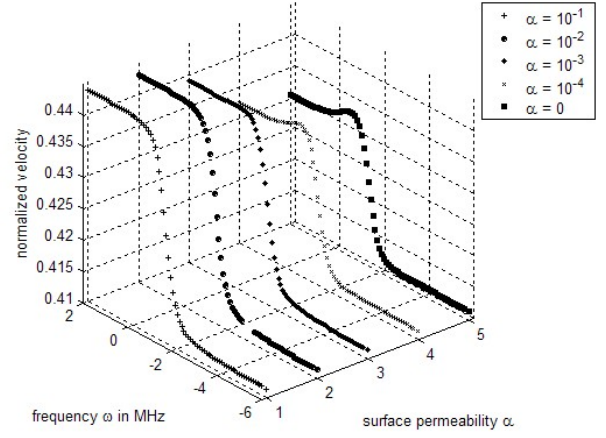


Figure 6: Boundary porous medium/fluid. Normalized velocity of the leaky Stoneley wave in dependence on the frequency and the surface permeability.

range. This may be an indication of the change of the Riemann surface which is, however, much better pronounced in the attenuations.

The velocity of the leaky Stoneley wave behaves similar to the Rayleigh wave. Also this wave possesses high an low frequency limits unequal to zero and the steep increase inbetween appears in the same frequency region. However, in contrast to the Rayleigh wave for this wave the high frequency limit is larger for bigger values of  $\alpha$  than for smaller ones. The frequency behavior of this wave is – at least for small  $\alpha$  – not monotonous. A maximum value appears in the region of order 100 kHz.

The true Stoneley wave exists only for small values of  $\alpha$ , and, therefore, we show its behavior only for two values of  $\alpha$ . For those the velocities do not differ substantially. They start form zero at  $\omega = 0$  and increase until around 100 kHz where they nearly reach a high frequency limit which is a little bit smaller than the velocity of the  $P2$  wave,  $c_f \equiv \frac{c_{P2}}{c_{P1}} = 0.4$ .

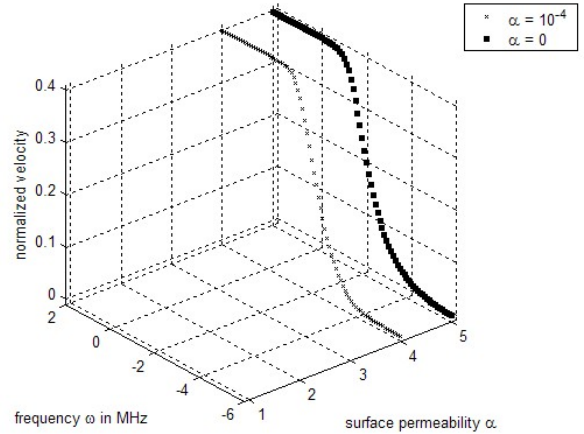


Figure 7: Boundary porous medium/fluid. Normalized velocity of the true Stoneley wave in dependence on the frequency and the surface permeability.



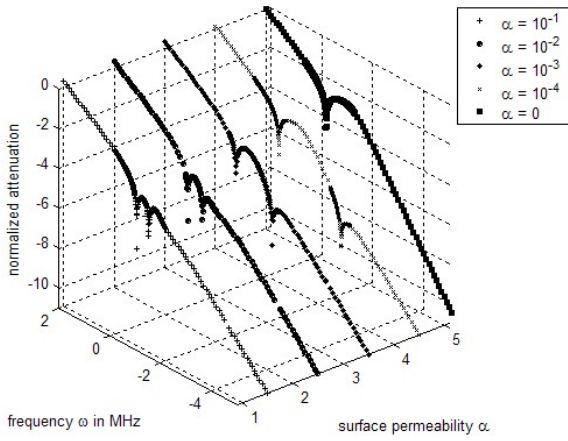


Figure 8: Boundary porous medium/fluid. Normalized attenuation of the leaky Rayleigh wave in dependence on the frequency and the surface permeability.

The attenuation of the true Stoneley wave has the same appearance as this obtained for the boundary porous medium/vacuum. We show a log-log-plot of this attenuation. It starts from zero as  $\omega = 0$  and nearly reaches a horizontal asymptote at around 100 kHz. In contrast to the true surface wave the remaining leaky waves possess singularities in the attenuation for two intermediate frequencies. These frequencies seem to be related with characteristic frequencies  $\frac{\pi}{2\rho_0^S}$  and  $\frac{\pi}{2\rho_0^F}$  which have already appeared in the stability analysis of adsorption processes (Albers 2003). However, there exists an influence of the parameter  $\alpha$ , responsible for dissipation, and, consequently, the location of the singularities changes with the variation of this coefficient. Hence, as indicated also in some papers on Biot's model, the diffusion-driven resonances appear also in the surface waves. Little is known about their mathematical origin. However, the numerical analysis indicates that they appear due to the change of the Riemann surface. In any case, it is obvious that the

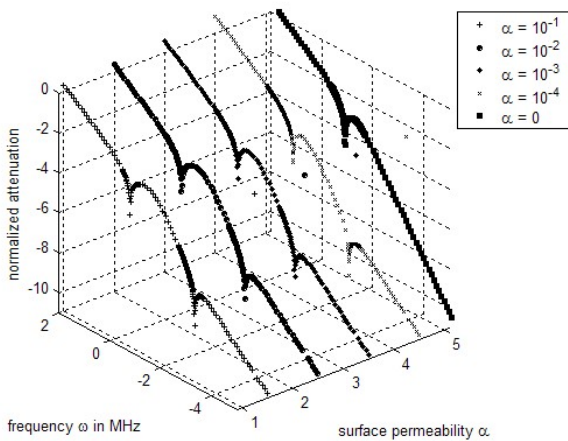


Figure 9: Boundary porous medium/fluid. Normalized attenuation of the leaky Stoneley wave in dependence on the frequency and the surface permeability.

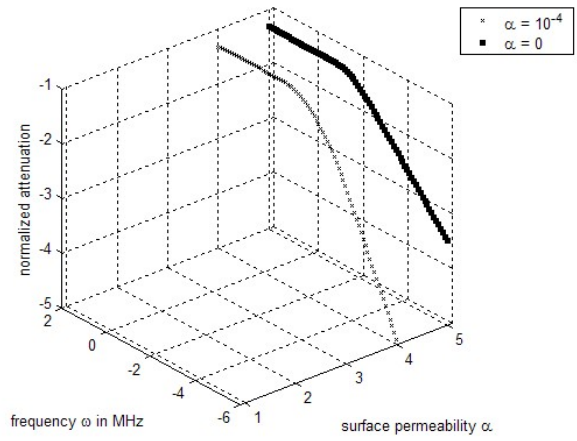


Figure 10: Boundary porous medium/fluid. Normalized attenuation of the true Stoneley wave in dependence on the frequency and the surface permeability.

curves show a leaky character.

## REFERENCES

- Albers, B. (2003). Relaxation analysis and linear stability vs. adsorption in porous materials. *Contin. Mech. Thermodyn.* 15(1), 73–95. also WIAS-Preprint Nr. 721, 2002.
- Albers, B. (2005). Modelling of surface waves in poroelastic saturated materials by means of a two component continuum. In C. Lai and K. Wilmanski (Eds.), *Surface Waves in Geomechanics: Direct and Inverse Modelling for Soils and Rocks*, CISM Courses and Lectures. Wien: Springer.
- Albers, B. and K. Wilmanski (2003a). Monochromatic surface waves on impermeable boundaries in two-component poroelastic media. Preprint 862, WIAS. to appear in: *Contin. Mech. Thermodyn.*
- Albers, B. and K. Wilmanski (2003b). On modeling acoustic waves in saturated poroelastic media. Preprint 874, WIAS. to appear in: *J. Engn. Mech.*
- Deresiewicz, H. and R. Skalak (1963). On uniqueness in dynamic poroelasticity. *Bull. Seismol. Soc. Am.* 53, 783–788.
- Feng, S. and D. L. Johnson (1983). High-frequency acoustic properties of a fluid/porous solid interface. I. New surface mode. *J. Acoust. Soc. Am.* 74(3), 906–914.
- Gubaidullin, A. A., O. Y. Kuchugurina, D. M. J. Smeulders, and C. J. Wisse (2004). Frequency-dependent acoustic properties of a fluid/porous solid interface. *J. Acoust. Soc. Am.* 116(3), 1474–1480.
- Wilmanski, K. (1999). Waves in porous and granular materials. In K. Hutter and K. Wilmanski (Eds.), *Kinetic and continuum theories of granular and porous media*, Number 400 in CISM Courses and Lectures, pp. 131–186. Wien New York: Springer.
- Wilmanski, K. (2004). Tortuosity and objective relative acceleration in the theory of porous materials. Preprint 922, WIAS. to appear in: *Proc. Royal Soc. (London), Ser. A.*
- Wilmanski, K. and B. Albers (2003). Acoustic waves in porous solid-fluid mixtures. In K. Hutter and N. Kirchner (Eds.), *Dynamic response of granular and porous materials under large and catastrophic deformations*, Volume 11 of *Lecture Notes in Applied and Computational Mechanics*, pp. 285–314. Berlin: Springer.